

Blue Glow Sticks: Cinnamic Acids and Arylacrylonitriles with Liquid-Crystalline Properties and Highly Fluorescent

Aline Tavares,^a Rebeca O. Costa,^{ib} Caroline S. B. Weber,^a Thiago Cazati,^{ib} Marco A. Ceschi,^a André A. Vieira^{ib}*,^b and Aloir A. Merlo^{ib}*,^a

^aInstituto de Química, Universidade Federal do Rio Grande do Sul, 91501-970 Porto Alegre-RS, Brazil

^bInstituto de Química, Universidade Federal da Bahia, 40170-115 Salvador-BA, Brazil

^cDepartamento de Física, Universidade Federal de Ouro Preto, 35400-000 Ouro Preto-MG, Brazil

Five new π -conjugated chromophores derived from acrylic acid and acrylonitrile were synthesized and their thermal and photophysical behaviors were analyzed. They were designed and synthesized through Knoevenagel condensations between arylacetylenebenzaldehydes and a methylene group activated from cyanoacetic and malonic acids. The characterization of the target compounds was performed by Fourier transform infrared spectroscopy (FTIR), ¹H nuclear magnetic resonance (NMR), ¹³C NMR, thermogravimetric analysis (TGA), absorption and emission spectroscopy techniques. Arylcinnamic acids were obtained as pure *E*-isomers. On the other hand, arylacrylonitrile was obtained as a mixture of *E/Z*-isomers and the pure *E*-isomer was isolated in chromatographic columns. The liquid crystal properties were investigated through differential scanning calorimetry and polarized optical microscopy. All chromophores displayed smectic and nematic mesophases. These materials displayed intense fluorescence under UV-Vis light excitation. The maximum absorption peaks were observed between 342-356 nm while emission varied from 428 to 460 nm in chloroform solution. Higher values for the quantum fluorescence yield were associated with acrylic acids compared to arylacrylonitriles. The solvatochromism studies of the materials showed a significant increase in the red-shift of the fluorescence spectra as the polarity of the solvent increased. In some cases, a variation in the emission wavelength from the blue to the green region of the spectrum was observed.

Keywords: Knoevenagel condensation, liquid crystal, fluorescence, quantum yields, solvatochromism

Introduction

Acrylic acid and acrylonitrile are important π -conjugated chromophores for manufacturing. As C3 chemical building blocks, they have the potential to provide several commodities for manufacturing polymers, medicines, cosmetics and food.¹ Their aryl derivatives are interesting chemicals for many functions and applications.²⁻⁴ Cinnamic acid and its derivatives are found in many natural products including coffee beans, tea, yerba mate and cocoa.⁵ Although arylacrylonitriles^{6,7} are less common in nature than cinnamic derivatives they are important molecule targets for synthesis, considering their wide range of promising biological properties.^{8,9} In academic and technological research they are used intensively in photoresponsive materials,¹⁰⁻¹² bowl-

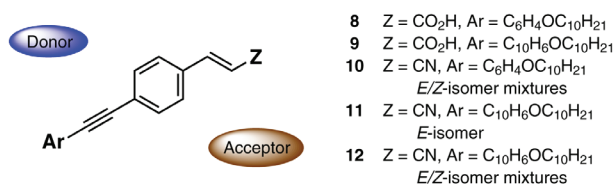
shaped fluorescent liquid crystals,^{13,14} H-bonded liquid crystals with enantiotropic blue phases,¹⁵ liquid crystal dimers,^{16,17} structure and mesomorphism correlations,¹⁸ hybrid liquid crystals,¹⁹ photodimerization reactions,²⁰ photoinduced orientation of liquid crystalline copolymer films by reversible addition-fragmentation chain transfer (RAFT) polymerization,²¹ photosensitive polyimide used in the photoalignment layer,²² photocrosslinkable thermotropic liquid crystal copolyesters²³ and piezochromic fluorophores.²⁴

One of the most famous families of π -conjugated chromophores, widely used in the field of functional organic materials, is that of the cyanostilbene chromophore, [-ArCH=C(CN)Ar-].^{25,26} π -Conjugated systems based on cyanostilbene and its derivatives represent a special family of chromophores in which the photophysical properties can be adjusted in response to a variety of external stimuli, such as viscosity, temperature, pressure, pH and light.^{27,28}

*e-mail: andreqmc@gmail.com; aloir.merlo@ufrgs.br

Elongated molecules containing electron-donor and acceptor groups connected by a bridge-like rigid arylacetylene group have a large extension of the electronic conjugation (structure donor- π linker-acceptor (D- π -A)), affording opportunities for exploration in the field of photoresponsive materials. In previous publications,^{13,19} cinnamic acid and its derivatives have been reported as important promoters of mesomorphism. However, for arylacrylonitriles the mesomorphism is less common or even absent. Moreover, due to the π -conjugated system photophysical features can be explored in parallel with liquid crystal properties.

In this study, we report the synthesis and characterization of five different rod-like molecules as a result of Knoevenagel condensation between aromatic aldehydes and activated methylene groups. Arylcinnamic acids were obtained as the pure *E*-isomers, while arylacrylonitriles were obtained as *E/Z*-isomer mixtures and the pure *E*-isomer was then isolated in chromatographic columns. The rigid π -conjugated core of these materials is composed of 4-*n*-alcoxydiphenylacetylene (tolane unit) or 6-*n*-alcoxyphenylphenyl-acetylene. The thermal and photophysical properties of all of the compounds were studied in order to investigate the structure-property relationships. The general molecular structure of the synthesized family of π -conjugated chromophores **8** and **9** (arylacrylic acid) and **10**, **11** and **12** (arylacrylonitrile) is shown in Scheme 1.



Scheme 1. General structure of compounds **8-12**.

Experimental

Materials and reagents

The solvents used in the chemical synthesis were purchased from commercial suppliers (Sigma-Aldrich Co, Pró-Análise Cia and Mercolab Cia; Porto Alegre, Brazil) and were purified according to common procedures.²⁹ Other chemicals and reagents were commercially available and used as received. Extracts were dried with anhydrous Na₂SO₄ and filtered before removal of the solvent by evaporation. The bis-(triphenylphosphine) palladium(II) chloride ([PdCl₂(PPh₃)₂]) was synthesized following a known procedure described in the literature.³⁰

Characterization

Proton and carbon nuclear magnetic resonance spectra (¹H and ¹³C NMR) were obtained with CDCl₃ as a solvent on a Varian 400 MHz spectrometer. Chemical shifts are given in parts *per million* (δ) and are relative to the signal of tetramethylsilane (δ 0 ppm for ¹H) as internal reference for solutions in CDCl₃. The NMR spectroscopic data are reported as follows: CDCl₃ (δ 7.26 ppm for ¹H or δ 77.1 ppm for ¹³C) and dimethyl sulfoxide (DMSO-*d*₆, δ 2.50 ppm for ¹H or δ 39.5 ppm for ¹³C). Multiplicities are reported according to the following abbreviations: s = singlet, d = doublet, t = triplet, q = quartet, m = multiplet, br = broad. Coupling constants (*J*) are given in Hz. Ultraviolet visible spectra (UV-Vis) of the 10⁻⁵ M solutions were obtained using a Varian Cary 50 UV/Vis Spectrophotometer. Fluorescence spectra were measured using a Shimadzu RF5301pc spectrofluorophotometer equipped with a xenon lamp and 1.0 cm quartz cells. The emission-slit widths were 5 and 5 nm, respectively. The characterization by Fourier transform infrared spectroscopy (FTIR) was measured using a Varian 640-IR spectrometer (KBr) between 4000 and 500 cm⁻¹ and with a resolution of 4 cm⁻¹. All spectra were performed with 16 scans and are given in wavenumbers (cm⁻¹). Low-resolution mass spectra (MS) were obtained with a Shimadzu GC-MS-QP5050 mass spectrometer interfaced with a Shimadzu GC-17A gas chromatograph equipped with a 30 meter Rtx-5MS (0.25 × 0.25 mm) capillary column. The column temperature started at 80 °C and held for 2 min, ramped to 250 °C at a rate of 10 °C min⁻¹, held for 2 min, ramped to 330 °C at 20 °C min⁻¹ and held for 10 min. The melting points, phase transition temperatures and mesomorphic textures were taken using an Olympus BX43 microscope equipped with a Mettler Toledo FP82HT Hot Stage with an FP90 Central Processor at a heating/cooling rate of 10 °C min⁻¹ (magnification: 10×). Carbon, hydrogen, and nitrogen (CHN) elemental analysis were performed on a PerkinElmer 2400 CHN Elemental Analyzer. Differential scanning calorimetry analyses (DSC) were performed on a Q2000 (TA instruments) with an ultra-pure nitrogen flow of 50 mL min⁻¹ with a heating rate of 10 °C min⁻¹ and Tzero aluminum hermetic pan. The thermal degradation was carried out by thermogravimetric analysis (TGA) on a TGA Discovery (TA Instruments) with an ultra-pure nitrogen flow of 25 mL min⁻¹ from 40 up to 500 °C with a heating rate of 10 °C min⁻¹ and platinum-HT pan.

Synthesis description

Synthesis of 4-[(4-decyloxyphenyl)ethynyl]benzaldehyde (**4**)
 Sonogashira's coupling: a one-neck round-bottom

flask equipped with septum stoppers was charged with dry NEt_3 (30 mL), 4-bromobenzaldehyde (**3**) (2.4 g, 13.0 mmol), alkyne **1** (5.0 g, 19.0 mmol), copper(I) iodide (CuI) (12.0 mg, 6.3×10^{-5} mol), triphenylphosphine (PPh_3) (76.0 mg, 2.9×10^{-4} mol) and bis-(triphenylphosphine) palladium(II) chloride ($[\text{PdCl}_2(\text{PPh}_3)_2]$) (40.0 mg, 5.8×10^{-5} mol, 0.3 mol%) under argon atmosphere. The mixture was heated under reflux for 48 h. After the suspension to reach room temperature, it was filtered through a Celite[®] pad and washed with CH_2Cl_2 . The filtrate was extracted with H_2O (3×50 mL) and the organic extracts were dried (Na_2SO_4) and evaporated off. The solid was recrystallized twice from ethanol and once from hexane affording the product. Yield: 3.6 g (77%) as a yellow solid; FTIR (KBr) $\nu_{\text{max}} / \text{cm}^{-1}$ 2951, 2918, 2846, 2738, 2210, 1699, 1597, 1514, 1282, 1244, 1205, 1068, 833, 680; ^1H NMR (400 MHz, CDCl_3) δ 0.91 (m, 3H, CH_3), 1.20-1.58 (m, 14H, $(\text{CH}_2)_7$), 1.81 (m, 2H, $\text{CH}_2\text{CH}_2\text{O}$), 4.00 (t, J 6.6 Hz, 2H, CH_2O), 6.91 (d, J 6.0 Hz, 2H, Ar), 7.50 (d, J 6.0 Hz, 2H, Ar), 7.66 (d, J 6.0 Hz, 2H, Ar), 7.87 (d, J 6.0 Hz, 2H, Ar), 10.02 (s, 1H, CHO); ^{13}C NMR (100 MHz, CDCl_3) δ 14.1, 22.7, 26.0, 29.1, 29.3, 29.4, 29.6, 31.9, 68.1, 87.4, 93.9, 114.2, 114.6, 129.6, 130.1, 131.8, 133.3, 135.0, 159.8, 191.4.

Synthesis of 4-[[6-decyloxynaphthalen)-2-yl]ethynyl] benzaldehyde (**5**)

Sonogashira's coupling: a one-neck round-bottom flask equipped with septum stoppers was charged with dry NEt_3 (30 mL), 4-bromobenzaldehyde (**3**) (2.0 g, 10.8 mmol), alkyne **2** (5.0 g, 16.0 mmol), copper(I) iodide (CuI) (10.0 mg, 5.2×10^{-5} mol), triphenylphosphine (PPh_3) (63.5 mg, 2.4×10^{-4} mol) and bis-(triphenylphosphine) palladium(II) chloride ($[\text{PdCl}_2(\text{PPh}_3)_2]$) (34.0 mg, 4.8×10^{-5} mol, 0.3 mol%) under argon atmosphere. The mixture was heated under reflux for 48 h. After the suspension to reach room temperature, it was filtered through a Celite[®] pad and washed with CH_2Cl_2 . The filtrate was extracted with H_2O (4×50 mL) and the organic extracts were dried (Na_2SO_4) and evaporated off. The solid was recrystallized twice from ethanol and once from hexane affording the product. Yield: 3.4 g (51%) as a yellow solid; FTIR (KBr) $\nu_{\text{max}} / \text{cm}^{-1}$ 2919, 2850, 1687, 1604, 1471, 1388, 1257, 1211, 1020, 862, 825; ^1H NMR (400 MHz, CDCl_3) δ 0.89 (m, 3H, CH_3), 1.20-1.58 (m, 14H, $(\text{CH}_2)_7$), 1.87 (m, 2H, $\text{CH}_2\text{CH}_2\text{O}$), 4.09 (t, J 6.6 Hz, 2H, CH_2O), 7.11-7.21 (m, 2H, Ar), 7.52-7.57 (m, 1H, Ar), 7.68-7.76 (m, 4H, Ar), 7.86-7.91 (m, 2H, Ar), 8.02 (s, 1H, Ar), 10.05 (s, 1H, CHO); ^{13}C NMR (100 MHz, CDCl_3) δ 14.3, 22.8, 26.2, 29.3, 29.4, 29.6, 29.7, 29.8, 32.1, 68.2, 88.4, 94.5, 106.7, 117.3, 120.1, 127.1, 128.4, 128.9, 129.5, 129.7, 130.0, 131.9, 132.1,

134.7, 135.3, 158.3, 191.5; MS (electrospray ionization (ESI)) m/z , $\text{C}_{29}\text{H}_{32}\text{O}_2$ [M^+]: 412.

Synthesis of *E*-3-[4-(4-decyloxyphenyl)ethynylphenyl] acrylic acid (**8**)

In a flask fitted with a reflux condenser was added the aldehyde **4** (2.5 g, 6.9 mmol), malonic acid (1.6 g, 15.0 mmol), pyridine (7 mL, 87.0 mmol), and piperidine (51 μL , 0.5 mmol) and refluxed for 2 days. After the solution cool down at room temperature, concentrated HCl was slowly added and the stirring continued for half an hour. The residue was filtered, washed with CH_2Cl_2 , and recrystallized twice from ethanol affording the product. Yield: 1.9 g (69%) as a yellow solid; FTIR (KBr) $\nu_{\text{max}} / \text{cm}^{-1}$ 3531, 2953, 2920, 2848, 1679, 1516, 1429, 1249, 1022, 985, 837, 653, 536; ^1H NMR (400 MHz, CDCl_3) δ 0.88 (m, 3H, CH_3), 1.16-1.52 (m, 14H, $(\text{CH}_2)_7$), 1.78 (m, 2H, $\text{CH}_2\text{CH}_2\text{O}$), 3.97 (t, J 6.4 Hz, 2H, CH_2O), 6.43 (d, 1H, J 16.0 Hz, $\text{HC}=\text{CH}$), 6.87 (d, 2H, J 8.4 Hz, Ar), 7.46 (d, 2H, J 8.4 Hz, Ar), 7.49 (s, 4H, Ar), 7.65 (d, 1H, J 16.0 Hz, $\text{HC}=\text{CH}$); elemental analysis calcd.: C 80.16, H 7.97, N 0.0%; found: C 79.94, H 7.99, N 0.11%.

Synthesis of *E*-3-{4-[(6-decyloxynaphthalen)-2-yl] ethynylphenyl}acrylic acid (**9**)

In a flask fitted with a reflux condenser was added the aldehyde **5** (312.0 mg, 0.7 mmol), malonic acid (141.0 mg, 1.7 mmol), pyridine (1 mL, 12.0 mmol), and piperidine (16 μL , 0.2 mmol) and refluxed for 2 days. After the solution cool down at room temperature, concentrated HCl was slowly added and the stirring continued for half an hour. The residue was filtered and washed with acetone and then purified by silica gel column (230-400 mesh (Merck)) using CH_2Cl_2 as eluent. The product was recovered washing the column with DMSO and isolated after crystallization in this solvent. Yield: 0.2 g (70%) as a white solid; FTIR (KBr) $\nu_{\text{max}} / \text{cm}^{-1}$ 3463, 2953, 2920, 2848, 1678, 1625, 1602, 1257, 1217, 1170, 985, 833, 663, 532; ^1H NMR (400 MHz, CDCl_3) δ 0.88 (m, 3H, CH_3), 1.16-1.56 (m, 14H, $(\text{CH}_2)_7$), 1.85 (m, 2H, $\text{CH}_2\text{CH}_2\text{O}$), 4.08 (t, J 6.3 Hz, 2H, CH_2O), 6.45 (d, 1H, J 16.2 Hz, $\text{HC}=\text{CH}$), 7.08-7.20 (m, 2H, Ar), 7.48-7.59 (m, 5H, Ar), 7.62-7.75 (m, 2H, Ar + 1H, $\text{HC}=\text{CH}$), 7.98 (s, 1H, Ar); elemental analysis calcd.: C 81.90, H 7.54, N 0.0%; found: C 81.36, H 7.23, N 0.16%.

Synthesis of mixture of *E* and *Z* isomers 3-[4-(4-decyloxyphenyl)ethynylphenyl]acrylonitrile (**10**)

In a flask fitted with a reflux condenser was added the acetonitrile (30 mL), aldehyde **4** (1.0 g, 2.7 mmol), cyanoacetic acid (283.0 mg, 3.3 mmol), and morpholine

(0.8 mL, 9.1 mmol) and refluxed for 3 days. After the solution cool down at room temperature a precipitate was formed. It was filtered, washed with hexane, recrystallized from CH₂Cl₂ and finally chromatographed on a silica gel column (230-400 mesh (Merck)) using hexane as eluent. The elution was monitored with UV-bench lamp illumination due to blue fluorescence of the compound in the column. Yield: 240 mg (23%) of the white solid as a mixture of *E/Z* (33:67); FTIR (KBr) ν_{\max} / cm⁻¹ 3064, 2920, 2852, 2214, 1595, 1514, 1473, 1286, 1249, 1136, 995, 810, 675, 538; ¹H NMR (400 MHz, CDCl₃) δ 0.88 (m, 3H, CH₃), 1.20-1.50 (m, 14H, (CH₂)₇), 1.78 (m, 2H, CH₂CH₂O), 3.97 (t, *J* 4.8 Hz, 2H, CH₂O), 5.45 (d, *J* 12.0 Hz, CH=CH, *Z*-isomer), 5.87 (d, *J* 16.0 Hz, CH=CH, *E*-isomer), 6.85 (d, *J* 8.8 Hz, 2H, Ar), 7.09 (d, *J* 12.0 Hz, CH=CH, *Z*-isomer), 7.37 (d, *J* 16.0 Hz, CH=CH, *E*-isomer), 7.41 (d, *J* 8.4 Hz, 2H, Ar), 7.45 (d, *J* 8.8 Hz, 2H, Ar), 7.52 (d, *J* 8.4 Hz, 2H, Ar), 7.55 (d, *J* 8.4 Hz, Ar, *Z*-isomer), 7.78 (d, *J* 8.4 Hz, Ar, *Z*-isomer); ¹³C NMR (100 MHz, CDCl₃) δ 14.0, 22.6, 25.9, 29.1, 29.2, 29.3, 29.5, 29.6, 31.8, 68.0, 87.4, 87.5 (*Z*-isomer), 92.4 (*Z*-isomer), 92.6, 95.0 (*Z*-isomer), 96.4, 114.3 (*Z*-isomer), 114.5, 117.2 (*Z*-isomer), 118.0, 126.3 (*Z*-isomer), 126.6, 127.2, 128.9, 131.6 (*Z*-isomer), 131.8, 132.5, 132.6 (*Z*-isomer), 133.0, 147.6 (*Z*-isomer), 149.5, 159.5.

Synthesis of (*E*)-3-[4-[(6-decyloxynaphthalen)-2-yl]ethynylphenyl]acrylonitrile (**11**) and (*E/Z*)-3-[4-[(6-decyloxy-naphthalen)-2-yl]ethynylphenyl]acrylonitrile (**12**)

In a flask fitted with a reflux condenser was added the acetonitrile (30 mL), aldehyde **5** (1.0 g, 2.4 mmol), cyanoacetic acid (250.0 mg, 2.9 mmol), and pyridine (0.5 mL, 6.2 mmol) and refluxed for 3 days. After the suspension cool down at room temperature, it was filtered and chromatographed on a silica gel column (230-400 mesh (Merck)) using hexane as eluent for one week. The elution was monitored with UV-bench lamp illumination: compound **11** has yellow fluorescence and eluted first and it was collected as pure *E*-isomer; compound **12** is yellow and has not fluorescence in the column, and it was collected as mixture of *E/Z* isomers (32:68). Yield: **11**, 200 mg (19%) as a yellow crystalline solid and **12**, 83 mg (8%) as a white crystalline solid.

Data for (*E*)-**11**

FTIR (KBr) ν_{\max} / cm⁻¹ 3064, 2920, 2852, 2216, 1600, 1469, 1386, 1257, 1213, 1166, 1020, 852, 817; ¹H NMR (400 MHz, CDCl₃) δ 0.89 (m, 3H, CH₃), 1.20-1.55 (m, 14H, (CH₂)₇), 1.85 (m, 2H, CH₂CH₂O), 4.07 (t, *J* 6.6 Hz, 2H, CH₂O), 5.88 (d, *J* 16.0 Hz, 1H, HC=CHCN), 7.10-7.21 (m, 2H, Ar), 7.38 (d, *J* 16.0 Hz, 1H, HC=CHCN), 7.43 (d,

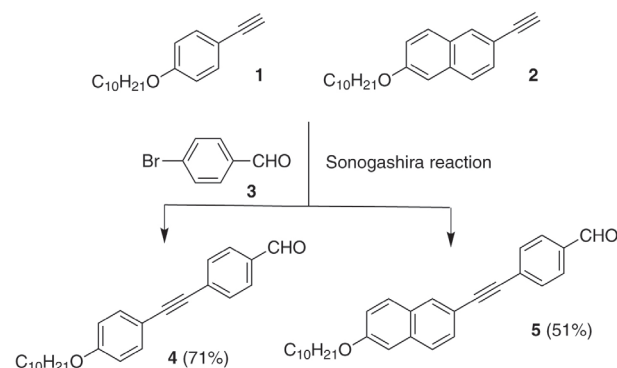
J 8.4 Hz, 2H, Ar), 7.50-7.60 (m, 3H, Ar), 7.65-7.74 (m, 2H, Ar), 7.98 (s, 1H, Ar); ¹³C NMR (100 MHz, CDCl₃) δ 14.1, 22.7, 26.1, 29.2, 29.3, 29.4, 29.5, 29.6, 31.9, 68.1, 88.3, 93.2, 96.7, 106.5, 117.3, 118.1, 119.9, 126.5, 126.9, 127.3, 128.3, 128.7, 129.3, 131.6, 132.1, 132.8, 134.4, 149.6, 158.1.

Data for (*E/Z*)-**12**

FTIR (KBr) ν_{\max} / cm⁻¹ 3062, 2920, 2852, 2218, 1600, 1469, 1386, 1257, 1213, 1166, 1022, 968, 856, 813; ¹H NMR (400 MHz, CDCl₃) δ 0.89 (m, 3H, CH₃), 1.20-1.55 (m, 14H, (CH₂)₇), 1.85 (m, 2H, CH₂CH₂O), 4.07 (t, *J* 6.6 Hz, 2H, CH₂O), 5.46 (d, *J* 12.0 Hz, HC=CHCN, *Z*-isomer), 5.88 (d, *J* 16.0 Hz, HC=CHCN, *E*-isomer), 7.10 (d, *J* 12.0 Hz, HC=CHCN, *Z*-isomer), 7.10-7.19 (m, 2H, Ar), 7.38 (d, *J* 16.0 Hz, HC=CHCN, *E*-isomer), 7.43 (d, *J* 8.0 Hz, 1H, Ar), 7.50-7.63 (m, 3H, Ar), 7.66-7.73 (m, 2H, Ar), 7.81 (d, *J* 8.4 Hz, 1H, Ar), 7.98 (m, 1H, Ar); ¹³C NMR (100 MHz, CDCl₃) δ 14.1, 22.6, 26.1, 29.2, 29.3, 29.4, 29.5, 29.6, 31.9, 68.1, 88.3 (*E*-isomer), 88.5 (*Z*-isomer), 92.9 (*Z*-isomer), 93.1 (*E*-isomer), 95.2 (*Z*-isomer), 96.6 (*E*-isomer), 106.5, 117.3 (*E*-isomer), 117.4 (*Z*-isomer), 118.0, 119.8 (*Z*-isomer), 119.9 (*E*-isomer), 126.2 (*Z*-isomer), 126.5 (*E*-isomer), 126.8 (*Z*-isomer), 126.9 (*E*-isomer), 127.3, 128.2 (*Z*-isomer), 128.3 (*E*-isomer), 128.7 (*E*-isomer), 128.8 (*Z*-isomer), 129.0 (*Z*-isomer), 129.3 (*E*-isomer), 131.6, 131.9 (*Z*-isomer), 132.1 (*E*-isomer), 132.8 (*E*-isomer), 132.9 (*Z*-isomer), 134.4 (*Z*-isomer), 134.5 (*E*-isomer), 147.7 (*Z*-isomer), 149.6 (*E*-isomer), 158.0 (*Z*-isomer), 158.1 (*E*-isomer).

Results and Discussion

Scheme 2 illustrates the synthetic route to obtain the aldehydes **4** and **5**. They were prepared in four steps according to a previously described methodology.³¹⁻³³ Alkynes **1** and **2** were prepared following methods already described in the literature³¹ and they were combined with

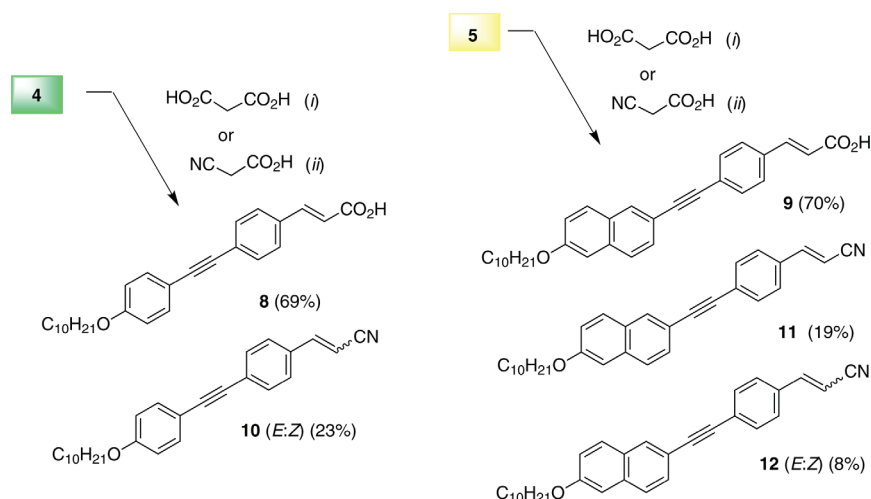


Scheme 2. Synthetic route to prepared **4** and **5**. Reaction conditions: NEt₃, CuI, PPh₃, [PdCl₂(PPh₃)₂], argon and reflux for 48 h.

bromobenzaldehyde (**3**) through the Sonogashira reaction to yield chromophores **4** and **5**.³¹⁻³³

Scheme 3 describes the synthesis of cinnamic acids and acrylonitrile derivatives. The installation of an electron-withdrawing group allows the effect of the acceptor fragment on thermal and photophysical properties of compounds **8-12** to be evaluated. All new compounds were satisfactorily characterized as described in the Experimental section. The final molecules were obtained by Knoevenagel condensation of aldehydes **4** or **5** in the following way: (i) cinnamic acid derivatives **8** and **9** were prepared by reaction of aldehyde **4** or **5** with malonic acid in the presence of piperidine and pyridine under heating for 2 days;³⁴ (ii) cyano derivatives **10**, **11**, and **12** were prepared by reacting cyanoacetic acid and aldehyde **4** or **5** in the presence of morpholine (or pyridine) in acetonitrile (reflux for 3 days).³⁵ The yields of the final compounds were determined after crystallization or by long and exhaustive chemical purifications through chromatographic columns. While **10** is a mixture of *E/Z*-isomers, compounds **11** and **12** were collected by chromatographic columns and characterized as *E*-isomer and *Z/E*-isomers, respectively. Compounds **11** and **12** were obtained from the same reaction vessel, and by a long and exhaustive separation process *E*-isomer was collected first and the second fraction collected was characterized as being *E/Z*-isomers. Attempts to separate *E/Z*-isomers from **10** has failed and it was analyzed as mixture of isomers. For Knoevenagel condensation to produce **10**, **11** and **12**, the aldehydes **4** and **5** were quite sluggish to react, giving unsaturated nitriles in low yields. Attempts to isolate pure (*E*)- α -cyanocinnamic acid have failed and a mixture of *E/Z*-cinnamionitrile was obtained, probably due to the prolonged treatment in boiling acetonitrile, which induces spontaneous decarboxylation of tetrahedral intermediate formed in the addition step.³⁵

The Knoevenagel condensation reactions showed different selectivity in the formation of the cinnamic acids **8** and **9** and acrylonitriles **10**, **11** and **12**. The reaction carried out with malonic acid was selective exclusively for the *E*-isomer configuration for **8** and **9**. The condensation reaction with cyanoacetic acid yielded a mixture of *E/Z* geometrical isomers. As discussed in the above paragraph, a fraction of pure *E*-isomer **11** was obtained by separation process from the *E/Z*-isomers mixture of **12**. The ¹H NMR spectra, recorded in CDCl₃ at room temperature, for compounds **9**, **11** and **12** are shown in Figure 1. The spectra for these final compounds show a very distinctive signal assigned to the vinylic protons. Compounds which showed a lower δ value for vinylic protons were assigned as *Z*-isomers and the other compounds as *E*-isomers. The spectrum of the *E*-isomer of **9** in Figure 1a shows doublets at δ 6.59 (H _{α}) and 7.62 ppm (H _{β}) with a typical coupling constant of *J* 16.2 Hz, related to the pure (*E*)-**9** isomer. In Figure 1b, the spectrum for the *E*-isomer of **11** has two doublets at δ 5.88 (H _{α}) and 7.38 ppm (H _{β}) with a coupling constant of *J* 16.0 Hz. Figure 1c shows the ¹H NMR spectrum for a mixture of *E/Z*-isomers of **12**. The *Z*-isomers display two doublets for vinylic protons at δ 5.46 (H _{α}) and 7.10 ppm (H _{β}) with a typical coupling constant of *J* 12.0 Hz. In the same spectrum there are also two additional doublets for *E*-isomers of the vinylic protons at δ 5.88 (H _{α}) and 7.38 ppm (H _{β}), with a typical coupling constant of *J* 16.0 Hz.³⁶ The integration of vinylic signals allowed the proportion of *E/Z*-isomers of sample **12** to be determined as 32% *E* and 68% *Z*-isomers. Thus, vinylic protons at high frequency (low field) refer to the *E*-isomer, while at low frequency (high field) they refer to the *Z*-isomer. This assignment is further confirmed by the ¹H NMR spectrum for the pure compound (*E*)-**11** without



Scheme 3. Reaction conditions for preparation of **8-12**: (i) CH₂(CO₂H)₂, piperidine, pyridine, reflux, 2 days; R = C₁₀H₂₁; (ii) NCCH₂CO₂H, morpholine, acetonitrile, reflux, 3 days.

its *Z*-isomer, where the *E*-vinylic protons appear as a doublet at δ 5.88 (H_α) and 7.38 ppm (H_β) (Figure 1b) with a coupling constant of J 16.0 Hz, confirming the correct assignment of the geometric isomers.^{36,37} In addition, the electron-withdrawing group effect is observed by comparing the pure isomers (*E*)-**11** and (*E*)-**9** in the ¹H NMR spectrum, as evidenced by the appearance of signals at high frequency for the *E*-isomer containing the carboxyl group and low frequency (high field) for the *E*-isomer of the nitrile group. The same analysis was applied to (*E*)-**8** and (*E/Z*)-**10** and compound **8** displayed doublets at δ 6.43 (H_α) and 7.65 ppm (H_β), while for **10** the *E*-isomer displayed two doublets at δ 5.87 (H_α) and 7.37 ppm (H_β) and *Z*-isomer showed doublets at δ 5.45 (H_α) and 7.10 ppm (H_β).

When compound **11** was subjected to the magnetic field in the ¹³C NMR analysis, the carbon atom of the –CN group appeared at 117.3 ppm while the corresponding carbon atom in the (*Z*)-**12** appeared at 117.4 ppm. In addition, the carbon atom of the olefinic group in the (*E*)-**12** appeared at 96.6 (C_α) ppm while corresponding carbon atom in (*Z*)-**12** appeared at 95.2 ppm (C_α). On the other hand, the other carbon atom of the olefin group of the molecule with (*Z*)-**12** appeared at 147.7 ppm (C_β), while the corresponding carbon atom in (*E*)-**12** appeared at 149.6 ppm (C_β). The assignment of the spectral data for the chromophores in this study is in accordance with that of similar compounds reported in the literature.³⁷

Liquid-crystal behavior

The transition temperatures of compounds **8-12** and intermediates **4-5** are summarized in Table 1. The transition temperatures, textures and images of the mesophase (Figure 2) were obtained using polarized optical microscopy (POM). DSC experiments were recorded for final samples. However, DSC traces in the first heating stage displayed the thermal history of the samples and attempts to perform the second and third heating/cooling cycles were unproductive due to thermal decomposition at high temperatures (above the clearing temperatures). Thus, the DSC data are not included in Table 1.

Table 1. Mesophases and transition temperatures for compounds **4, 5, 8, 9, 10, 11** and **12** upon heating

Compound	Transition temperature / °C
4	Cr 85 I
5	Cr 111 N 135 I
8	Cr 206 SmC 260 N dec. I
9	Cr 220 SmC 278 N dec. I
10	Cr 89 SmA 159 I
11	Cr 110 SmA 152 N 185 I
12	Cr 101 SmA 163 N 198 I

Data were recorded by POM. Cr: crystal phase; I: isotropic phase; N: nematic mesophase; SmA and SmC: smectic A and C mesophase.

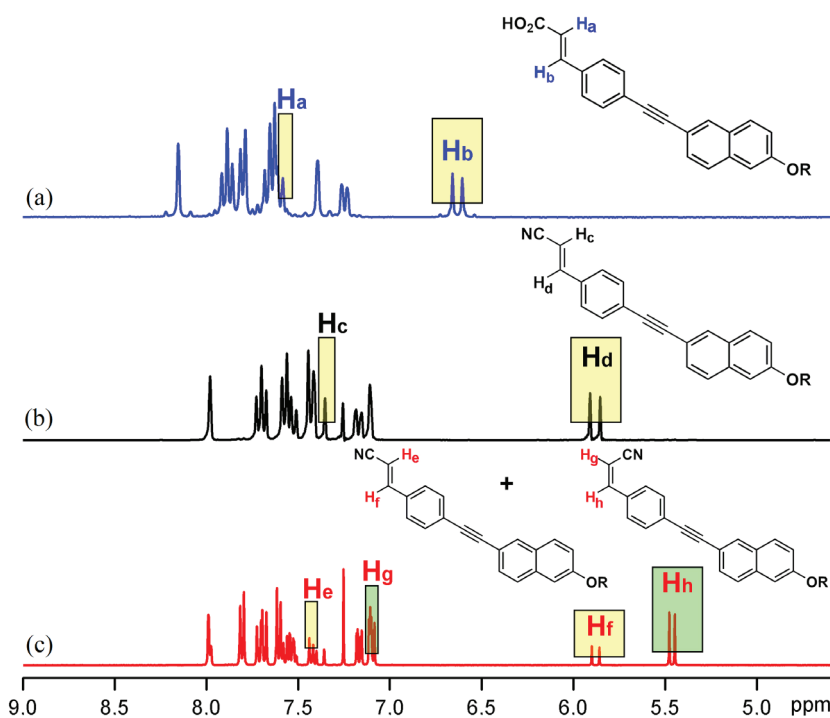


Figure 1. Magnification of a region of the ¹H NMR spectra (400 MHz, CDCl₃) for compounds (a) **9** (*E*-isomer); (b) **11** (*E*-isomer); (c) **12** (32% of *E* and 68% of *Z*-isomers).

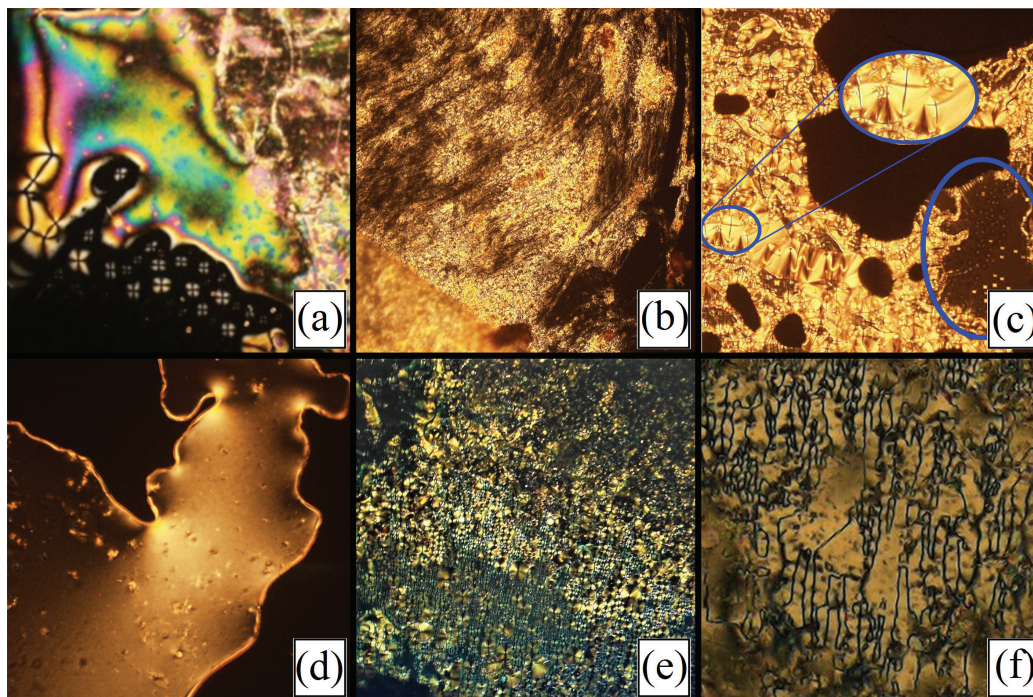


Figure 2. POM images of the compounds: (a) **5** (schlieren texture, at right, two- and four-fold disclination lines; at left, marble texture; and some Maltese cross below, for nematic phase, upon heating at 134 °C); (b) **9** (blurred schlieren texture for SmC mesophase, upon heating to 226 °C); (c) **10** (fan-focal conic texture for SmA mesophase along black and irregular air bubbles, upon cooling to 148 °C. Focal-conic domains (FCDs) present optical discontinuities, being visible in ordinary light and with crossed polarized, and they appear as dark lines. The dark lines form the ellipses and hyperbole in the conics geometry, which are highlighted in Figure 2c. In a special case, FCDs can display an ellipse as a circle and hyperbole as straight line); (d) **11** (nematic phase with flashing effect, phase director instabilities, upon cooling to 166 °C. Under no stress conditions, samples appear completely black in the interior and colorful in the neighborhood); (e) **12** (fan-focal conic and radial textures for SmA mesophase, upon cooling to 145 °C); (f) **12** (planar texture for nematic phase, upon heating to 175 °C).

In general, aldehyde **4** did not exhibit a mesophase, aldehyde **5** showed enantiotropic liquid-crystal behavior with a nematic phase when analyzed by POM (Table 1 and Figure 2a). Cinnamic acids **8** and **9** showed nematic and smectic C (SmC) mesophases in the POM analysis, with the mesomorphism range largely dependent on the arylacetylene group. As noted for cinnamic acids **8** and **9**, as well as the acrylonitriles **10**, **11** and **12**, the naphthylacetylene group favors the mesophase range more than the phenylacetylene group by increasing the length/width ratio. Another aspect that should be emphasized is the thermal behavior at high temperatures. We noted visually in the POM analysis that the compounds of both series (cinnamic acids and acrylonitriles) started to decompose when they reached the liquid phase at high temperature. Images of the mesophase are generally taken upon cooling from the isotropic state to eliminate residual structural information present in the ordered phase and to capture good quality pictures. Thus, in the liquid state, no information about the order of the system is available and when the sample transits from the isotropic phase to a mesophase some degree of order is added, for instance, orientational order for the nematic phase or translational order for the smectic phase. The texture observed originates

from the imperfections of the samples or the glass responsible for the creation of the defects of the phase, which is the texture observed under cross polarized light.

Aldehyde **5** displayed a nematic mesophase (N) (Figure 2a) in contrast with **4**, which has no mesophase. Compounds **8** and **9** presented high melting and clearing temperatures. Upon heating, **8** melted at 180 °C while **9** melted at 221 °C. Both solids became an anisotropic fluid displaying blurred schlieren texture under heating, suggesting an SmC mesophase, which is present but not clearly observed in Figure 2b. At very high temperatures (> 260 °C) the nematic mesophase was quickly observed from the schlieren texture. The temperature associated with the transition to the isotropic phase was not registered due to the decomposition of the samples at high temperatures.

For the arylacrylonitrile **10**, an elongated rod-shaped molecule with a mixture of *E/Z*-isomers displayed stable smectic A (SmA) with a mesophase range of 70 °C. From the isotropic phase, **10** entered into the SmA mesophase at 148 °C and crystallized at 72 °C (Figure 2c). Investigation of the pure *E*-isomer of **11** revealed SmA and N mesophases. Upon heating, compound **11** entered into the SmA mesophase at 110 °C with a fan-focal conic texture, and at 152 °C the sample entered into the

N mesophase with planar texture and at 185 °C reached the isotropic liquid phase. On cooling from the isotropic phase, **11** displayed a homeotropic texture at 190 °C, as observed in the POM analysis, with characteristic black domains, homeotropic alignment with flashing effects, fast and reversible orientational movements of the phase director (*n*) (Figure 2d), typical of a nematic phase. The last acrylonitrile (**12**) was analyzed as a mixture of *E/Z*-isomers and showed enantiotropic SmA and N mesophases. Upon heating, SmA starts at 101 °C and with further heating up to 163 °C it transits into the N mesophase, finally melting into an isotropic liquid at 198 °C. Fan-focal conic and radial textures as well as planar nematic textures for the SmA and N mesophase, respectively, are seen in Figures 2e and 2f.

The polar-ended group also has an effect on the liquid crystal properties, as seen for **4**, **8** and **10**, which all have same aromatic core. However, the carbonyl group in **4** is a less efficient polar group, in terms of the mesophase stabilization, than the carboxyl group (by dimers) in **8** or the cyan group (directional dipolar orientation) in **10**. The liquid crystal behavior of a mixture of isomers (*E/Z*)-**10** and (*E/Z*)-**12** with the pure isomer (*E*)-**11** can be observed from the data in Table 1. Comparing the isomers with the naphthylacetylene group, pure *E*-isomer **11** displays higher melting point than *E/Z*-isomer **12**. Clearing temperature for the *E/Z*-isomer is 13 °C above the *E*-isomer **11**. The result here reveals that packing considerations are more important for pure isomer (*E*)-**11**, as expected. However, anisotropic interactions favor the mesophase range for (*E/Z*)-**12**, especially for SmA mesophase through lateral diffusion,³⁸ probably due to the excess of *Z*-isomer over *E*-isomer in **10** and **12**. Another point is related to the length-to-breadth ratio, which is crucial to the thermal stability of the mesophase. The naphthyl group in this class of molecules is a better stabilizer group than phenyl, due to the breadth supplied by naphthyl moieties, as evidenced by the mesophase range, melting point and clearing temperature in Table 1. Thus, in this series, the mesophase stability follows the order: naphthylacetylene group > phenylacetylene group (tolane unit)^{31,32} and others.³⁹

Thermal stability of organic compounds

The thermal properties of cinnamic acids **8** and **9** and acrylonitrile **10** and **12** were investigated by TGA under N₂ atmosphere to determine exactly when the decomposition phenomena occurs. Figure 3 shows two degradation peaks in the thermogravimetry-derivative thermogravimetry (TG-DTG) curves, which correspond to degradation of the material in two steps in the range of 50 to 500 °C. For **10** and **8** the second peak is less intense than in the case of

12 and **9**. While **10** and **8** contain alkoxyphenylacetylene units, alkoxyphenylacetylene is present in **12** and **9**. Above 500 °C, the residual solid that remains is higher for the compounds that contain the naphthalene ring in their structure.

The TG-DTG curves for compounds **8** and **9** displayed two weight loss peaks, as seen in Figures 3a and 3b. For compound **8**, the weight loss of around 70% in the region of 210-360 °C is related to the elimination of cinnamic acid and the decyloxy chain. The weight loss between 384 and 500 °C (around 14%) could be assigned to a loss of volatile materials from residual material that remains above 500 °C. For **9**, it can be seen from Figure 3b that the first degradation process occurs in the region of 235-385 °C with weight loss of around 15%, which is related to butenoic acid elimination. The weight loss between 385 and 500 °C (around 21%) could be assigned to loss of the phenyl group. The remaining residue (around 64%) is material resulting from the decomposition above 500 °C. For acrylonitrile **10**, the first degradation peak in Figure 3c is in the region of 250-380 °C, with the weight loss of around 68% related to the elimination of the cinnamionitrile and decyl groups. The weight loss between 400 and 500 °C (around 16%) could be assigned to the loss of low molecular weight volatiles, such as water for phenylacetylene, and above 500 °C a residual material (char) remains. In the case of **12** (Figure 3d), the peaks on the TG-DTG curves in the region of 280-390 °C may be related to a weight loss of around 39% associated with the decyloxy chain. The weight loss between 390 and 500 °C (around 18%) could be assigned to the elimination of the acrylonitrile unit. The residue (around 40%) is a char material composed of high molecular weight materials derived from naphthylphenylacetylene.

Photophysical properties, absorption and fluorescence

The photophysical properties of compounds **8-12** and intermediates **4-5** are shown in Table 2. Absorption and fluorescence spectra were taken in diluted solutions of chloroform (10⁻⁵ M) and the representative spectra are given in Figure 4. All molecules exhibited absorption between 300 and 400 nm, with maxima close to 340 nm. These absorption bands are assigned to π - π^* transitions due to their high molar absorption coefficients ($\epsilon = 3.0$ - 6.8×10^4 L mol⁻¹ cm⁻¹). The naphthyl group in the rigid core clearly shifted the absorbance of the compounds to longer wavelengths (ca. 10 nm) when compared to phenyl systems. The terminal groups showed bathochromic shifts in the following order: acrylonitrile > carboxylic acid > aldehyde, according to the nature of the withdrawing effect of these groups.

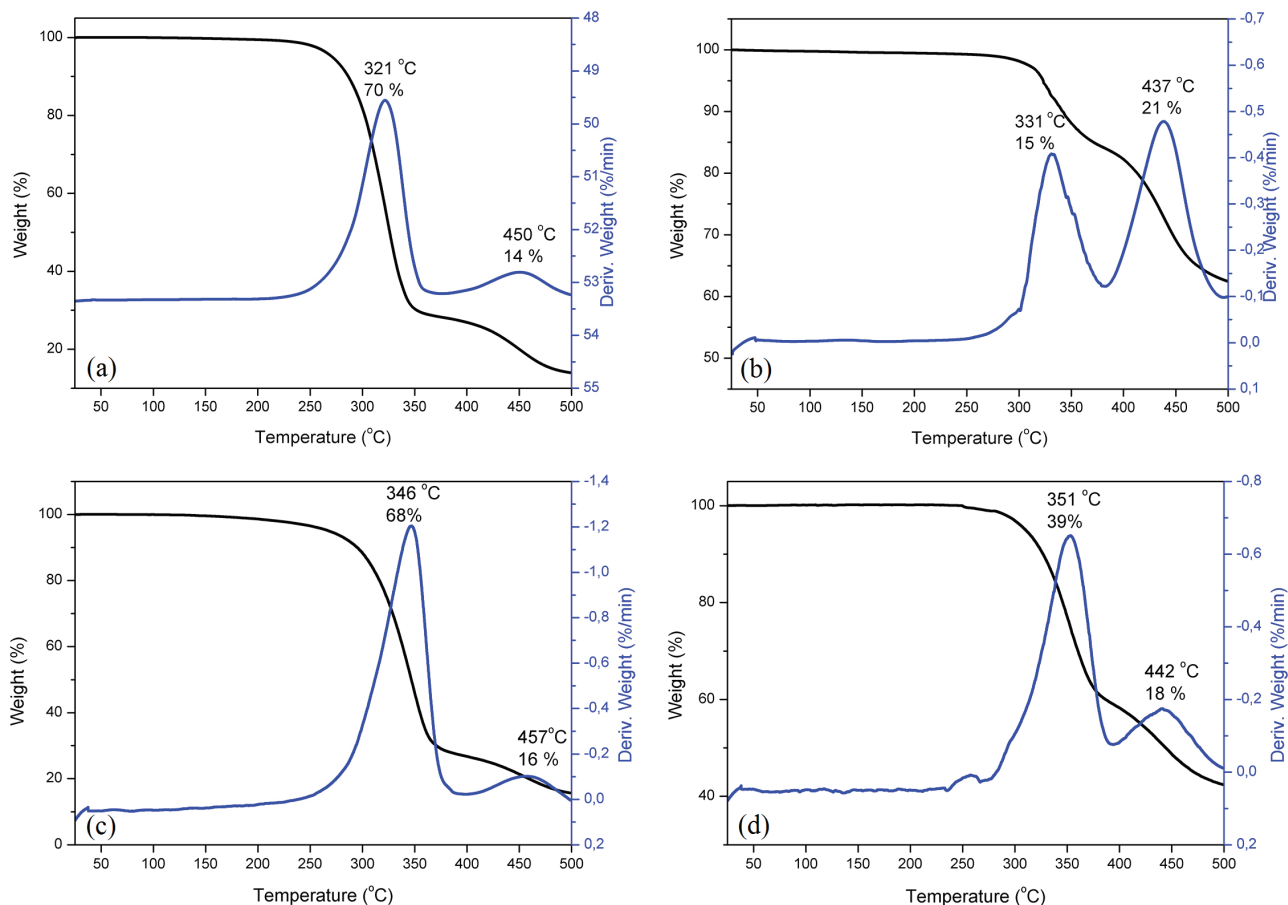


Figure 3. TG and DTG thermograms of compounds (a) **8**; (b) **9**; (c) **10** and (d) **12** (N_2 flow of 25 mL min^{-1} with a heating rate of $10 \text{ }^\circ\text{C min}^{-1}$).

Table 2. Summary of photophysical properties of **4**, **5** and **8-12** compounds

Sample	$\lambda_{\text{max}} / \text{nm}$		Stokes shift / cm^{-1}	Φ_{PL}^c
	Absorption ^a ($\epsilon / (10^4 \text{ L mol}^{-1} \text{ cm}^{-1})$)	Emission ^{a,b}		
4	340 (4.3)	428	6047	0.07
5	349 (5.3)	452	6529	0.50
8	342 (3.2)	444	6717	0.87
9	352 (3.0)	460	6670	0.99
10	346 (4.4)	428	5537	0.79
11	356 (6.7)	448	5768	0.86
12	356 (6.8)	448	5768	0.78

^aChloroform solution ($1.5 \times 10^{-5} \text{ mol L}^{-1}$); ^bexcited at maximum absorption; ^cdetermined using quinine sulfate as standard ($\Phi_{\text{Fl}} = 0.546$ in $1 \text{ M H}_2\text{SO}_4$). ϵ : molar absorption coefficient; Φ_{PL} : fluorescence quantum yields.

All compounds exhibited intense fluorescence when excited at the maximum absorption wavelength in solution. Emission peaks were observed from 428 to 460 nm. Once again, for the molecules with naphthyl groups (**5**, **9** and **11**) the peaks were at longer wavelengths when compared to the phenyl systems (Figure 4).

With respect the terminal groups, a hypsochromic shift in the maximum emission wavelength is observed with the replacement of the carboxylic acid group with

the cyan group in both phenyl and naphthyl systems. The carboxylic acids **8** and **9** show maximum emission at 444 and 460 nm, respectively, while the acrylonitriles **10** and **11** present emission at 428 and 448 nm. This phenomenon may be related to the more intense electron withdrawing effect of the cyan group. The *E*-isomer **11** showed exactly the same maxima of absorbance and emission as the mixture of *E:Z* geometrical isomers **12**. The Stokes shifts are in the range of 88-140 nm ($5537\text{-}6717 \text{ cm}^{-1}$) with a small

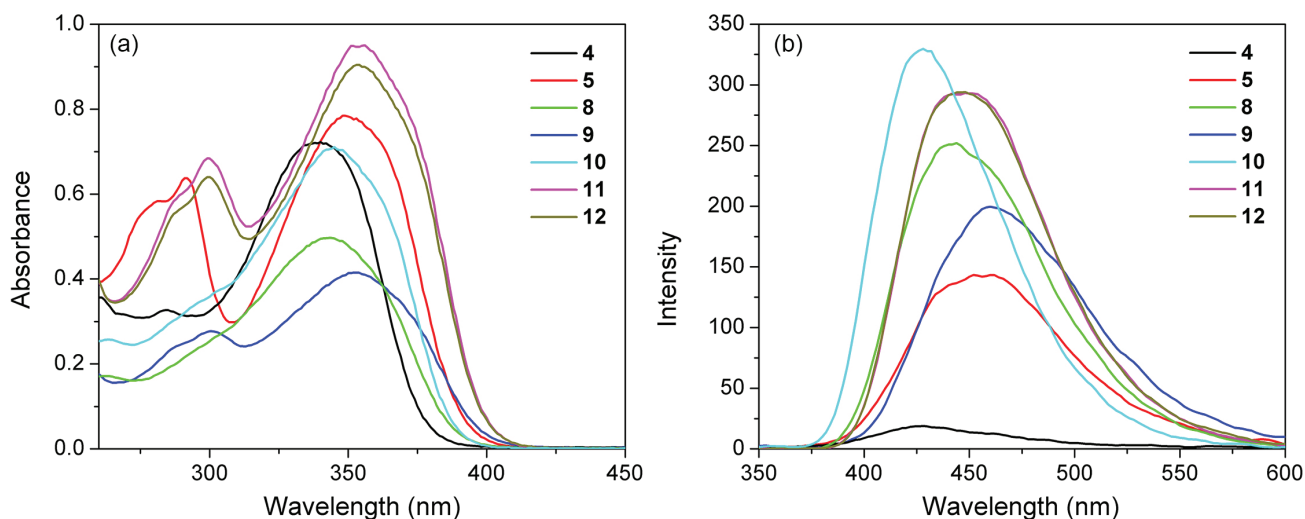


Figure 4. Absorbance (a) and emission (b) spectra for compounds **4**, **5** and **8-12** in chloroform solution (10^{-5} mol L $^{-1}$).

region of coincidence between the absorption and emission. The molecules exhibited fluorescence quantum yields (Φ_{PL}) of between 0.07 and 0.99 relative to the standard quinine sulfate (Table 2).⁴⁰ In general, the naphthyl derivatives (**5**, **9**, **11**) showed higher quantum yields when compared to the phenyls (**4**, **8**, **10**), probably due the greater π -extended conjugation. The phenyl- (**4**) and naphthyl-aldehyde (**5**) intermediates exhibited the lowest quantum yields of the series (0.07 and 0.50, respectively). On the other hand, the photoluminescence efficiency of the carboxylic acids **8** and **9** was slightly higher than that of the acrylonitrile derivatives (0.87 and 0.99, respectively). Through the photophysical study it was possible to observe that the *E*-isomer of acrylonitrile (**11**) presented a superior quantum yield than the *E:Z* mixture (**12**).

Solvatochromism properties

In order to investigate the solvatochromic properties of the compounds, the absorption and fluorescence spectra of **8**, **9** and **11** were obtained in diluted solutions of heptane, acetone, acetonitrile, chloroform, dimethylformamide, tetrahydrofuran, toluene, ethyl acetate and ethanol.⁴¹ The optical properties were measured in heptane, acetone, acetonitrile, chloroform, dimethylformamide (DMF), tetrahydrofuran (THF), toluene, ethyl acetate and ethanol solutions. Figure 5 shows the normalized emission spectra for sample **11** in solvents of different polarities and their optical data are summarized in Table 3. Small spectral variations are observed for the absorption spectra of these samples regardless of the polarity of the solvents. However, a significant increase in the red-shift of the fluorescence spectra as the polarity solvent increases was observed. The maximum emissions of compound **11** were shifted

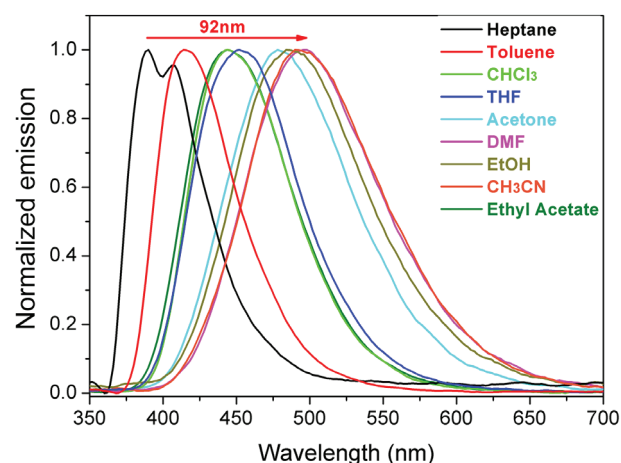


Figure 5. Normalized emission spectra for acrylonitrile **11** in different solvents.

Table 3. Absorption and emission data for compound **11** in different solvents

Solvent	$\lambda_{max} / \text{nm}$		Stokes shift / cm^{-1}
	Absorption ^a ($\epsilon / (\text{L mol}^{-1} \text{cm}^{-1})$)	Emission ^b	
Heptane	350 (1.0×10^4)	402	3696
Toluene	352 (3.4×10^4)	416	4371
CHCl ₃	353 (6.7×10^4)	450	6106
THF	349 (3.6×10^4)	454	6627
Acetone	344 (3.4×10^4)	480	8236
DMF	349 (3.3×10^4)	492	8328
CH ₃ CN	346 (3.0×10^4)	494	8659
EtOH	348 (2.1×10^4)	488	8244
Ethyl acetate	346 (3.3×10^4)	446	6480

^aSolution concentration = (1.5×10^{-5} mol L $^{-1}$); ^bexcited at maximum absorption. ϵ : molar absorption coefficient; THF: tetrahydrofuran; DMF: dimethylformamide.

from 402 (heptane) to 494 nm (acetonitrile), representing a variation of 92 nm.

The increase in the red-shift of the fluorescence spectra or the Stokes' shift as the polarity solvent increases is consistent with the stabilization of the excited states by the polar solvents.⁴² This process, called solvent relaxation, indicates that the excited state of these compounds is more polar than the ground state. Similar behavior of absorption and emission spectra were observed for compounds **8** and **9**. These samples also presented emission bands shifted to longer wavelengths with an increase in the solvent polarity.

The influence of solvent polarity on the optical properties of a fluorophore can be estimated using the Lippert-Mataga equation.^{43,44} The plot of the Stokes shifts ($\Delta\nu$) as a function of orientation polarizability (Δf) for **11** is shown in Figure 6. The increase in $\Delta\nu$ with an increase in the solvent polarity parameter leads to a linear correlation of 0.976.

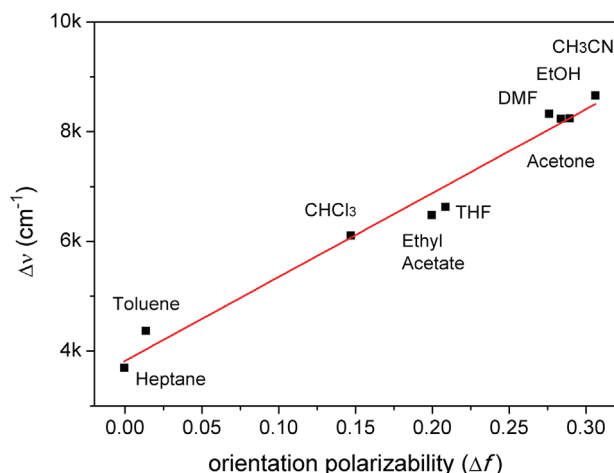


Figure 6. Changes in the Stokes shifts ($\Delta\nu$) of **11** versus Δf of various solvents.

The calculated values for the slope of the linear correlation for these compounds showed that the slopes became steep in the order of **11** (15300 cm^{-1}) > **8** (12300 cm^{-1}) > **9** (12900 cm^{-1}). These results indicate that the optical properties of these compounds show different degrees of solvent dependence and for these samples, the acrylonitrile **11** exhibits the steepest slope, indicating the largest fluorescence solvatochromism.

Conclusions

In summary, we prepared new derivatives of acrylic acids **8** and **9** and acrylonitriles **10**, **11** and **12**. Compounds **10** and **12** were isolated as a mixture of *Z/E*-isomers while the other compounds were characterized as pure *E*-isomers. Chromophores displayed N, SmA and SmC mesophases, and mesophase range for chromophores was dependent on

the nature of arylacetylene group. Despite of enantiotropic mesophase range, the main drawback are their relatives high melting point and thermal decomposition above $250 \text{ }^\circ\text{C}$ as noted for **8** and **9**, that limit for practical applications. Photophysical properties of the final compounds were influenced by the phenyl and naphthyl units, as well as the peripheral groups. These molecules exhibited strong blue fluorescence with maxima between 428 and 460 nm and significant quantum yields (0.78-0.99) in solution. The solvatochromism studies showed that the excited state of these compounds is more polar than their ground state, which led to a red-shift of the fluorescence spectra as the solvent polarity increased. The photophysical results reported herein make these systems promising candidates to be applied in optoelectronic devices.

Supplementary Information

Supplementary data (^1H NMR, ^{13}C NMR and FTIR spectra) are available free of charge at <https://jbc.sbj.org.br> as PDF file.

Acknowledgments

We are grateful to MCTI/CNPq for Ed. Universal grant number 403075/2016-5 and 422750/2018-2, FAPERGS Edital PqG 002/2014 for grant number 2280-2551/14-0, and FAPESB (PIBIC) for financial support. This study was financed in part by the Coordenação de Aperfeiçoamento de Pessoal de Nível Superior, Brazil (CAPES), finance code 001.

Author Contributions

Aline Tavares, Caroline S. B. Weber, Marco A. Ceschi were responsible for the investigation, data curation, formal analysis (synthesis, spectral and thermal data); Rebeca O. Costa, Thiago Cazati, André A. Vieira for the investigation, data curation, formal analysis (UV and fluorescence data); Aloir A. Merlo for the conceptualization, project administration, resources; André A. Vieira and Aloir A. Merlo also were responsible for writing original draft, review and editing.

References

- Guzman, J. D.; *Molecules* **2014**, *19*, 19292.
- Martínez-Abadía, M.; Robles-Hernández, B.; de la Fuente, M. R.; Giménez, R.; Ros, M. B.; *Adv. Mater.* **2016**, *28*, 6586.
- Shanker, G.; Rao, D. S.; Prasad, S. K.; Yelamagad, C. V.; *Tetrahedron* **2012**, *68*, 6528.

4. Guo, H.; Lin, L.; Qiu, J.; Yang, F.; *RSC Adv.* **2017**, *7*, 53316.
5. Clifford, M. N.; *J. Sci. Food Agric.* **1999**, *79*, 362.
6. Jimenez, D. E. Q.; Zanin, L. L.; Diniz, L. F.; Ellena, J.; Porto, A. L. M.; *Curr. Microwave Chem.* **2019**, *6*, 54.
7. Magarian, E. O.; Nobles, W. L.; *J. Pharm. Sci.* **1969**, *58*, 1167.
8. Parveen, M.; Malla, A. M.; Alam, M.; Ahmad, M.; Rafiq, S.; *New J. Chem.* **2014**, *38*, 1655.
9. Briguglio, I.; Laurini, E.; Pirisi, M. A.; Piras, S.; Corona, P.; Fermeglia, M.; Pricl, S.; Carta, A.; *Eur. J. Med. Chem.* **2017**, *141*, 460.
10. Praveen, P. L.; Ojha, D. P.; *J. Mol. Liq.* **2012**, *169*, 110.
11. Kumavat, P. P.; Baviskar, P. K.; Sankapal, B. R.; Dalal, D. S.; *New J. Chem.* **2016**, *40*, 634.
12. Percino, M. J.; Chapela, V. M.; Pérez-Gutiérrez, E.; Cerón, M.; Soriano, G.; *Chem. Pap.* **2011**, *65*, 42.
13. Sharma, V. S.; Singh, H. K.; Sharma, A. S.; Shah, A. P.; Shah, P. A.; *New J. Chem.* **2019**, *43*, 15575.
14. Lu, H.; Zhang, S.; Ding, A.; Yuan, M.; Zhang, G.; Xu, W.; Zhang, G.; Wang X.; Qiu, L.; Yang, J.; *New J. Chem.* **2014**, *38*, 3429.
15. He, W.-L.; Wei, M.-J.; Yang, H.; Yang, Z.; Cao, H.; Wang, D.; *Phys. Chem. Chem. Phys.* **2014**, *16*, 5622.
16. Bholá, G. N.; Maheta, R. H.; Bhoya, U. C.; *Mol. Cryst. Liq. Cryst.* **2015**, *623*, 129.
17. Shankerz, G.; Yelamaggad, C. V.; *New J. Chem.* **2012**, *36*, 918.
18. Muniya, N. R.; Patel, V. R.; *Mol. Cryst. Liq. Cryst.* **2016**, *638*, 77.
19. da Rosa, R. R.; Tariq, M.; Weber, C. S. B.; Hameed, S.; Silva, S.; Merlo, A. A.; *Liq. Cryst.* **2016**, *43*, 1659.
20. D'Auria, M.; Racioppi, R.; *Tetrahedron* **1997**, *53*, 17307.
21. Kawatsuki, N.; Matsuda, T.; Kondo, M.; *Mol. Cryst. Liq. Cryst.* **2010**, *529*, 10.
22. Kim, S. Y.; Shin, S. E.; Shin, D. M.; *Mol. Cryst. Liq. Cryst.* **2010**, *520*, 116/[392].
23. Wei, P.; Wang, Y.; Xia, Y.; He, Y.; Wang, Y.; *Liq. Cryst.* **2019**, *46*, 176.
24. Kunzelman, J.; Kinami, M.; Crenshaw, B. R.; Protasiewicz, J. D.; Weder, C.; *Adv. Mater.* **2008**, *20*, 119.
25. An, B.-K.; Gierschner J.; Park, S. Y.; *Acc. Chem. Res.* **2012**, *45*, 544.
26. Yoon, S.-J.; Kim, J. H.; Kim, K. S.; Chung, J. W.; Heinrich, B.; Mathevet, F.; Kim, P.; Donnio, B.; Attias, A.-J.; Kim, D.; Park, S. Y.; *Adv. Funct. Mater.* **2012**, *22*, 61.
27. Zhu, L.; Zhao, Y.; *J. Mater. Chem. C* **2013**, *1*, 1059.
28. Martínez-Abadía, M.; Robles-Hernandez, B.; Villacampa, B.; de la Fuente, M. R.; Gimenez, R.; Ros, M. B.; *J. Mater. Chem. C* **2015**, *3*, 3038.
29. Perrin, D. D.; Armarego, W. L. F.; *Purification of Laboratory Chemicals*, 3rd ed.; Pergamon Press: Oxford, 1988.
30. King, A. O.; Negishi, E.; Villani Jr., F. J.; Silveira Jr., A.; *J. Org. Chem.* **1978**, *43*, 358.
31. Tavares, A.; Ritter, O. M. S.; Vasconcelos, U. B.; Arruda, B. C.; Schrader, A.; Schneider, P. H.; Merlo, A. A.; *Liq. Cryst.* **2010**, *37*, 159; Merlo, A. A.; Tavares, A.; Khan, S.; Santos, M. J. L.; Teixeira, S. R.; *Liq. Cryst.* **2018**, *45*, 310.
32. Vasconcelos, U. B.; Merlo, A. A.; *Synthesis* **2006**, *7*, 1141; Tavares, A.; Arruda, B. C.; Boes, E. S.; Stefani, V.; Stassen, H. K.; Campo, L. F.; Bechtold, I. H.; Merlo, A. A.; *J. Braz. Chem. Soc.* **2012**, *23*, 880.
33. Vasconcelos, U. B.; Dalmolin, E.; Merlo, A. A.; *Org. Lett.* **2005**, *7*, 1027; Tavares, A.; Toldo, J. M.; Vilela, G. D.; Gonçalves, P. F. B.; Bechtold, I. V.; Kitney, S. T.; Kelly, S. M.; Merlo, A. A.; *New J. Chem.* **2016**, *40*, 393.
34. Pawar, H. S.; Wagh, A. S.; Lali, A. M.; *New J. Chem.* **2016**, *40*, 4962; Brand, Y. M.; Kouznetsov, V. V.; Puerto, C. E.; Linares, V. C. R.; Castaño, V. T.; Betancur-Galvis, L.; *J. Braz. Chem. Soc.* **2020**, *31*, 999.
35. Jones, G.; *Org. React.* **2011**, 204; Ziarani, G. M.; Moradi, R.; Lashgari, N.; Kruger, H. G.; *Metal-Free Synthetic Organic Dyes*; Elsevier Inc.: Amsterdam, 2018, p. 109; Ziarani, G. M.; Moradi, R.; Lashgari, N.; Kruger, H. G.; *Metal-Free Synthetic Organic Dyes*; Elsevier Inc.: Amsterdam, 2018, p. 197; Feng, Q.; Zhang, Q.; Lu, X.; Wang, H.; Zhou, G.; Wang, Z.-S.; *ACS Appl. Mater. Interfaces* **2013**, *5*, 8982; Wada, S.; Suzuki, H.; *Tetrahedron Lett.* **2003**, *44*, 399; Sharma, Y. O.; Degani, M. S.; *Green Chem.* **2009**, *11* 526; Wilk, M.; Trzepizur, D.; Koszelewski, D.; Brodzka, A.; Ostaszewski, R.; *Bioorg. Chem.* **2019**, *93*, 102816.
36. Ruan, J.; Li, X.; Saidi, O.; Xiao, J.; *J. Am. Chem. Soc.* **2008**, *130*, 2424; Fang, F.; Li, Y.; Tian, S.-K.; *Eur. J. Org. Chem.* **2011**, *2011*, 1084.
37. Andrus, M. B.; Song, C.; Zhang, J.; *Org. Lett.* **2002**, *4*, 2079; Kojima, S.; Fukuzaki, T.; Yamakawa, A.; Murai, Y.; *Org. Lett.* **2004**, *6*, 3917.
38. Fritsch, L.; Baptista, L. A.; Bechtold, I. H.; Araújo, G.; Mandle, R. J.; Merlo, A. A.; *J. Mol. Liq.* **2020**, *298*, 111750.
39. Prajapati, A. K.; Patel, H. N.; *Liq. Cryst.* **2007**, *34*, 903 and references cited therein; Kihara, H.; Tamaoki, N.; *Liq. Cryst.* **2007**, *34*, 1337; Dave, J. S.; Vora, R. A.; *Mol. Cryst. Liq. Cryst.* **1971**, *14*, 319.
40. Fery-Forgues, S.; Lavabre, D.; *J. Chem. Educ.* **1999**, *76*, 1260.
41. Marini, A.; Muñoz-Losa, A.; Biancardi, A.; Mennucci, B.; *J. Phys. Chem. B* **2010**, *114*, 17128.
42. Monçalves, M.; Zanotto, G. M.; Toldo, J. M.; Rampon, D. S.; Schneider, P. H.; Gonçalves, P. F. B.; Rodembush, F. S.; Silveira, C. C.; *RSC Adv.* **2017**, *7*, 8832.
43. Lakowicz, J. R.; *Principles of Fluorescence Spectroscopy*; Springer: New York, USA, 2006.
44. Noboru, M.; Yozo, K.; Masao, K.; *Bull. Chem. Soc. Jpn.* **1956**, *29*, 465.

Submitted: May 19, 2020

Published online: August 7, 2020

